Pis'ma v ZhETF, vol. 99, iss. 11, pp. 754 – 759 © 2014 June 10

Neutron scattering study of reduced graphene oxide of natural origin

E. F. Sheka[+1)], *I. Natkaniec*[*×], *N. N. Rozhkova*[°], *K. Holderna-Natkaniec*[×]

[+]*Peoples' Friendship University of Russia, 117198 Moscow, Russia*

[*]*Frank Laboratory of Neutron Physics, Joint Institute for Nuclear Research, 141980 Dubna, Russia*

[×]*Department of Physics, Adam Mickiewicz University, 61-712 Poznań, Poland*

[°]*Institute of Geology, Karelian Research Centre of the RAS, 185610 Petrozavodsk, Russia*

Submitted 31 March 2014
Resubmitted 5 May 2014

The current paper presents a direct confirmation of graphene-like configuration and first suggests the chemical composition of basic structural elements of shungite attributing the latter to reduced graphene oxide nanosize sheets with an average 11:1:3 (C:O:H) atomic content ratio.

DOI: 10.7868/S0370274X14110083

High-yield production of few-layer graphene flakes from graphite is important for the scalable synthesis and industrial application of graphene. Graphene-based sheets show promise for a variety of potential applications, and researchers in many scientific disciplines are interested in these materials. Although many ways of generating single atomic layer carbon sheets have been developed, chemical exfoliation of graphite powders to graphene oxide (GO) sheets followed by deoxygenation to form chemically modified reduced graphene oxide (rGO) has been so far the only promising route for bulk scale production. However, available technologies face a lot of problems among which there are low yield, the potential fire risk of GO and rGO when alkaline salt byproducts are not completely removed, a great tendency to aggregation, a large variety of chemical composition, and so forth (see the latest exhaustive reviews [1, 2] and references therein). In light of this, the existence of natural rGO is of utmost importance due to not only lower costs but unprecedented chemical stability provided by the geological long-term stabilization. As shown recently [3], shungite carbon from the deposits of carbon-rich rocks of Karelia (Russia) [4] presents a multilevel fractal structure based on nanoscale rGO sheets. This suggestion was the result of a careful analysis of physico-chemical properties of shungite widely studied to date as well as was initiated by knowledge accumulated by the current graphene science. Since then, two new direct justifications of the suggestion have been obtained. The first one is related to the study of photoluminescence (PL) of shungite aqueous and organic dispersions [5] that exhibits properties similar to those of synthetic graphene quantum dots of the rGO origin of nanometer size [6]. The second was obtained in the course of the neutron scattering study presented in the current paper.

Neutron scattering study was performed at the high flux pulsed IBR-2 reactor of the Frank Laboratory of Neutron Physics of JINR by using the NERA spectrometer [7]. The investigated samples are illuminated by white neutron spectrum analyzed by time-of-flight method on the 110 m flight path from the IBR-2 moderator. The inverted-geometry spectrometer NERA allows simultaneously recording both Neutron Powder Diffraction (NPD) and Inelastic Neutron Scattering (INS) spectra. The INS spectra are registered at final energy of scattered neutrons fixed by beryllium filters and crystal analyzers at $E_f = 4.65$ meV. Three powdered shungite samples were subjected to the study. The first pristine shungite Sh1 presents natural material of the highest carbon content from the Shun'ga deposit (see a detailed description of stability of the material properties in [4]). The second shungite Sh2 is a modified Sh1 after lengthy drying at 110 °C. The third shungite Sh3 is a solid condensate of colloids of the shungite Sh1 aqueous dispersions. Powdered spectral graphite was used to register both the reference NPD and INS spectra from pure carbon material.

As shown in Fig. 1, the general NPD patterns of all shungite samples are identical and similar to that of spectral graphite while drastically differ from the latter by shape: all Gr(hkl) peaks are upshifted and considerably broadened pointing to irregular structure of the shungites. As seen in the figure, the narrow peak

[1)]e-mail: sheka@icp.ac.ru

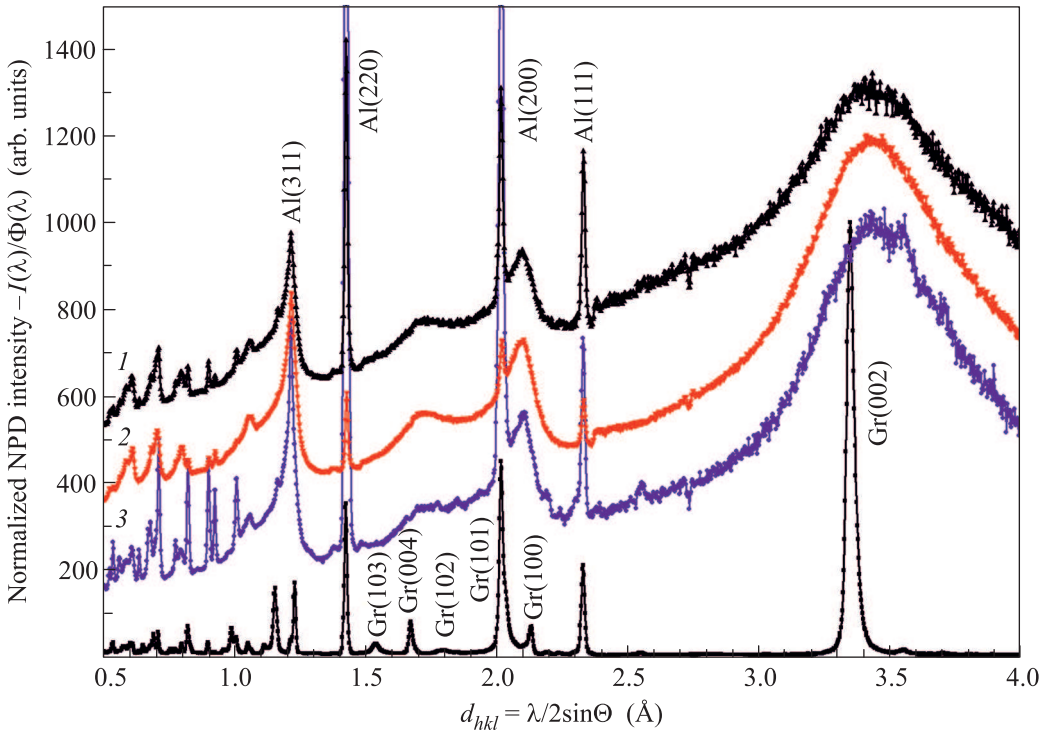

Fig. 1. NPD of spectral graphite (Gr) and shungites Sh1 (*1*), Sh2 (*2*), and Sh3 (*3*) recorded at $T = 20$ K. Scattering angle $2\Theta = 117.4^\circ$. The data are normalized per neutron flux intensity $\Phi(\lambda)$ at each neutron wave length λ, next, intensity of both shungite and graphite peaks in the Gr(002) region are normalized to 1000 arbitrary units; Gr(*hkl*) and Al(*hkl*) denote characteristic diffraction peaks of spectral graphite and cryostat aluminum at different Miller indexes, respectively

Gr(002) of graphite, the shape and width of which correspond to the resolution function of spectrometer and whose position determines d_{002} interfacial distance between the neighboring graphite layers, is substituted with broad peaks. The slight upshift of the peaks convincingly evidences a conservation of the graphite-like structure of all the shungite samples while the peaks wide broadening tells about a considerable space restriction.

A well known Scherrer equation, due to which the length $L_{\rm CSR}$ of the coherent scattering region (CSR) is inversely connected: $B = k\lambda/L_{\rm CSR}\sin\Theta$, where λ and Θ are of diffracting flux wave length and scattering angle, has been used when studying nanostructured graphites for a long tome [8]. Applying to shungites, it is possible to determine $L_{\rm CSR}$ by using the reference $L_{\rm CSR} \sim 20$ nm for spectral graphite alongside with the known ratio of FWHMs of the relevant diffraction peaks. The obtained value constitutes 1.3 nm, accuracy of which depends on how accurate are the reference data that may be quite widely spread due to which the obtained $L_{\rm CSR}$ value can be considered as a certain evaluation. Nevertheless, the obtained $L_{\rm CSR}$ value is quite coherent with those of 2.18 and 2.30 nm for Sh1 and Sh3, respectively, obtained by X-Ray diffraction [9]. Within the framework of shungite multilevel fractal structure [3], there might be two size limitations that correlate with the obtained $L_{\rm CSR}$ values: these are: 1) the linear dimension of individual rGO sheets (~ 1 nm) and 2) the thickness of the sheet graphite-like stacks that form the first level of the shungite structure. Summarizing NPD and X-Ray data, $L_{\rm CSR}$ of $\sim 1.5-2$ nm can be suggested as a reasonable average estimation. The latter implies $\sim 5-6$ layers of ~ 1 nm rGO fragments in the stacks.

INS spectra of Sh1 and Sh2 are given in Fig. 2. The spectrum of Sh3, scaled in accordance with the mass ratio, is quite identical to that of Sh1. Two pristine spectra presented in the figure clearly exhibit strong scattering from both samples in contrast with that from graphite thus indicating that both shungites are evidently hydrogen-enriched. At the same time, the two spectra differ in both intensity and shape. Since Sh2 was produced from Sh1 by lengthy heating, which was followed by removing water previously retained in Sh1, the difference spectrum *1–2* in the figure evidently presents the spectrum of released water. Actually, well known characteristic features of the INS water spectrum are clearly observed in the spectrum of Sh1 while no traces

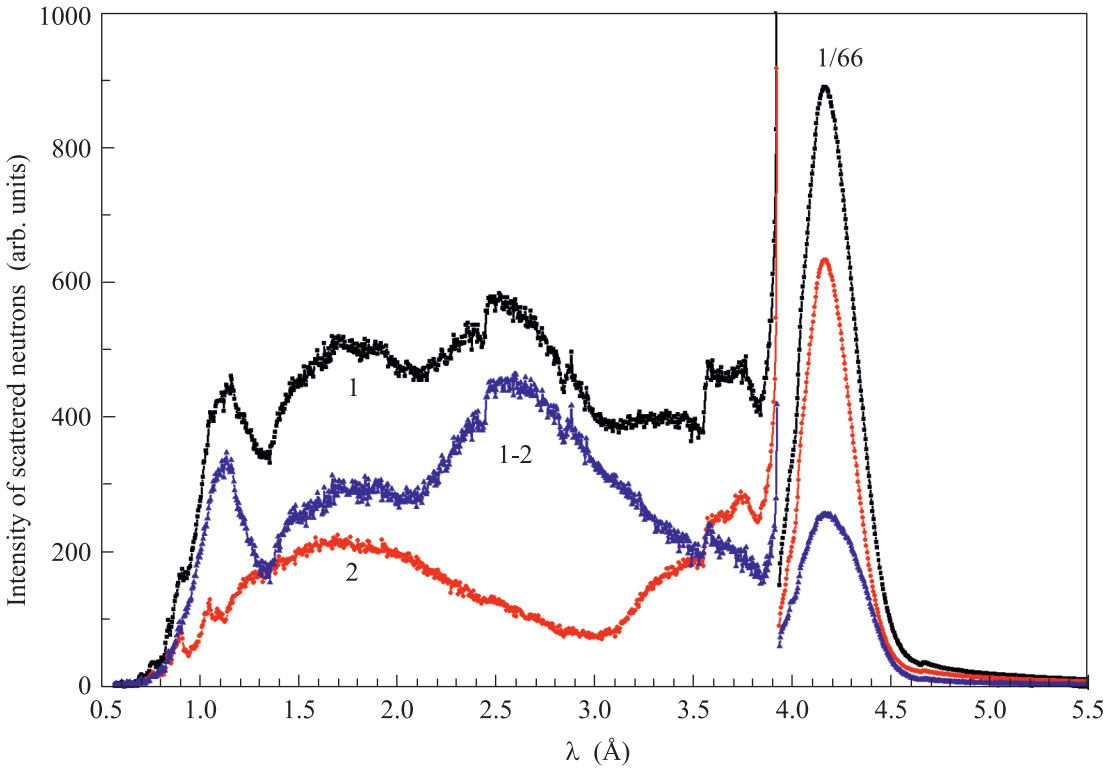

Fig. 2. Time-of-flight INS spectra of shungites Sh1 (*1*) and Sh2 (*2*) at 20 K after extraction of the INS spectrum of spectral graphite that is indistinguishable from the background. Spectra are normalized per 10^6 monitor counts of incident neutrons. Curve *1*, *2* presents the difference between spectra *1* and *2*. The intensity of elastic peaks is 66-fold reduced

of such structure are seen in the spectrum of Sh2. At the same time, the latter is quite intense, which undoubtedly points to the presence of hydrogen atoms incorporated in the carbon structure of shungite. The presence of the hydrogen atoms in the core of dried shungite has been directly observed for the first time.

To proceed with a detailed analysis of the obtained spectra, let us move on to the consideration of the density of vibrational states. The relevant $G(\omega)$ spectra of one-phonon amplitude-weighted density of vibrational states (AWDVS) are shown in Fig. 3 (see details of $G(\omega)$ spectra obtaining in [10]). Three main features follow from the general overview of the spectra. The first concerns spectrum *1–2* in Fig. 3b that can be evidently considered as the spectrum $G^{\rm wat}(\omega)$ of retained water. The spectrum presents the contribution of 4 wt % water in the spectrum $G^{\rm Sh}(\omega)$ of the pristine shungite and is pretty similar to those well known for retained water in silica gels [11, 12], Gelsil glasses [13], oxygenated graphite [14], and various zeolites [15]. The second feature is related to the evident absence of the retained water crystallization so that the $G^{\rm wat}(\omega)$ spectrum represents the bound water [14], molecules of which are connected with the solid shungite ground via hydrogen bonds and are located within the first adlayer. The third feature is related to the spectrum *2* in Fig. 3a that evidently exhibits the presence of hydrogen in the shungite core. The relevant $G^{\rm core}(\omega)$ spectrum differs drastically from the water one and is identical to the INS spectrum of a synthetic rGO [16] thus directly confirming the rGO nature of shungite. The spectrum is characterized by a considerable flattening up to 500 $\rm cm^{-1}$ and reveals a pronounced structure in the region of 600–1200 $\rm cm^{-1}$. The total intensity of $G^{\rm core}(\omega)$ spectrum constitutes approximately 1/3 of the $G^{\rm wat}(\omega)$ one. Taking into account that the latter is provided by 4 wt % water, it is possible to evaluate 1.8 wt % mass content of hydrogen in the shungite core. The data well correlate with 1.5±0.5 wt % hydrogen that was obtained by a thorough analysis of the chemical composition of synthetic rGO [17, 18].

As known, water molecules can be retained either on the surface of solid nanoparticles (see adsorbed water on aerosil [12]) and interfacial region of layered nanostructures [14] or in pores formed by the bodies [12–15]. The multi-layer graphene structure of shungites with interfacial spacing of ∼3.45 Å leaves no possibility of introducing 1.75 Å-thick water molecules between the layers. The latter can be accommodated either on the outer

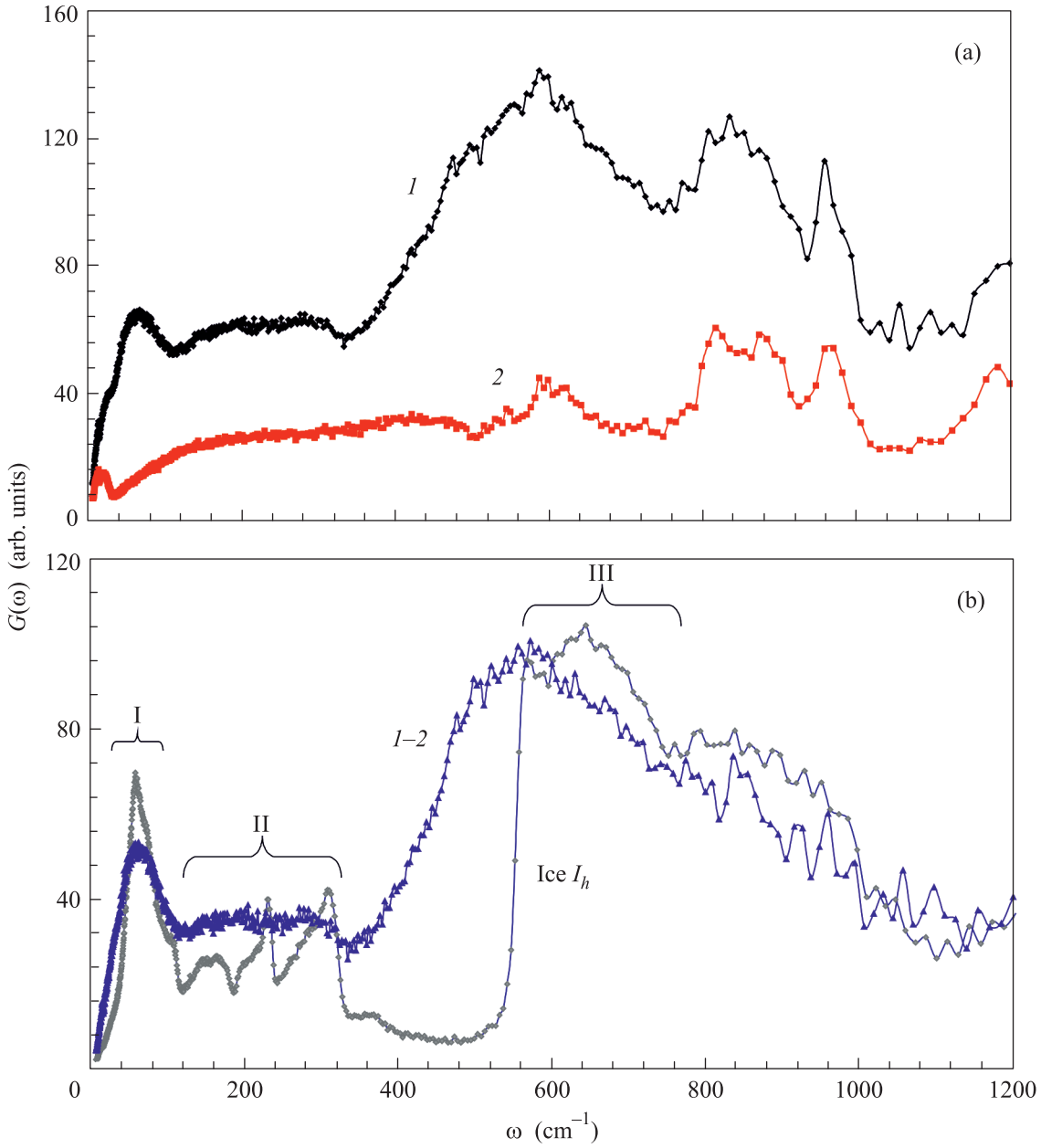

Fig. 3. (a) – One-phonon AWDVS spectra of Sh1 ($G^{\mathrm{Sh}}(\omega)$; 1) and Sh2 ($G^{\mathrm{core}}(\omega)$; 2). (b) – The difference spectrum (*1–2*) ($G^{\mathrm{wat}}(\omega)$) and spectrum of I_h ice ($G^{\mathrm{ice}}(\omega)$); $T = 20\,\mathrm{K}$

surface of $\sim 1.5{-}2$ nm shungite stacks or in pores made of the latter and their aggregates. Small angle neutron scattering (SANS) from shungite [19], which was possible precisely because of its hydrogen-enriched structure, exhibited pores of 2–10 nm and >20 nm in size thus pointing the place of the water accommodation. This explains a very deep similarity that is observed between the AWDVS spectra of the water retained in pores of silica gels [11, 12], Gelsil glass [13], and $G^{\mathrm{wat}}(\omega)$ spectrum of shungites.

The two-mode hydrogen composition of the pristine shungite opens the way to clear the chemical covering of pore walls. According to the modern concept of shungite structure [3], the pores are mainly covered with oxygen atoms of carbonyl units complemented by a small portion of hydroxyls [20]. However, as it has been noted even earlier [3], the relevant oxygen contribution is high, which contradicts with real data indicating a few wt % of oxygen or less. Moreover, as follows from the $G^{\mathrm{core}}(\omega)$ spectrum in Fig. 3a, clearly vivid maxima at

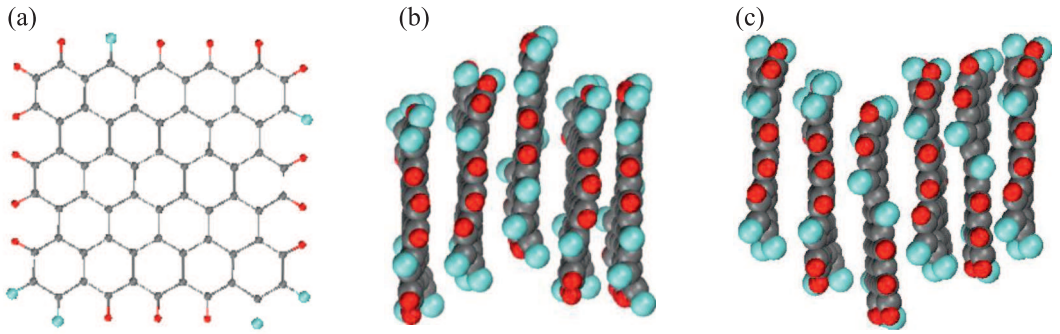

Fig. 4. (Color online) (a) – Equilibrium structure of ~ 1 nm (5, 5) rGO sheet corresponding to a strong reduction of the pristine (5, 5) GO sheet (see [21] for details). (b, c) – Arbitrary models of five- and six-layer rGO stacks with 3.5 Å interlayer distance. Gray, blue, and red balls present carbon, oxygen, and hydrogen atoms

~ 610, 820, 880, 960, and 1200 cm^{-1} fall in the region of the most characteristic non-planar deformational vibrations of the alkene C–H bonds. The finding convincingly points to the presence of C–H bonds in the circumference of rGO nanosheets thus exhibiting a *post-factum* hydrogenation of the pristine rGO. This hydrogenation plays a determining role in the hardness of the reduction process placing the latter between soft and hard ones as limiting cases. A thorough analysis of the hydrogenation reaction resulted in the formation of hydrogenated rGO, is discussed in [21]. Taking into account empirically known average size ~ 1 nm of the shungite rGO fragments and basing on 1.8 wt % hydrogen in the studied sample determined in the current study, a reasonable model of the atomic structure of shungite rGO, shown in Fig. 4a, can be suggested. Relating to the chemical composition of the sheet involving 66 carbon atoms in total, 22 atoms of which are located in the circumference area, its chemical formula can be presented as $C_{66}O_6H_{16}$, in particular, or $\sim C_{11}O_1H_3$, in general, that might be attributed to hard reduced rGO sheets of any size and shape. This composition is compatible with the hydrogen content of Sh2 revealed in the current study as well as with experimental data on the atomic and mass content of synthetic hard reduced rGO [17, 18, 21].

As for the retained water, it is well known that in the low-frequency region (0–1000 cm^{-1}), the INS spectrum of bulk water $G^{\rm ice}(\omega)$ shows a hindered translational spectrum (I and II in Fig. 3b) convoluted with the low-frequency Debye phonon-like acoustical contribution and a librational spectrum (III). Both the hindered translational and rotational (librations) modes of water are caused by intermolecular hydrogen bonds (HB). All these features are collective in character; thus it is quite natural to expect a strong spectral modification passing from the bulk to retained state, which is clearly seen in Fig. 3b. Thus, the only ice mode positioned at ~ 56 cm^{-1} (HB bending) is retained in the $G^{\rm wat}(\omega)$ spectrum while ~ 150 cm^{-1} (HB bending) as well as ~ 224 and ~ 296 cm^{-1} (HB stretchings) ice modes reveal clearly seen flattening and downshift. Analogous spectral modification takes place with respect to the ice librational modes forming a broad band in the region of 600–1200 cm^{-1}. The band is provided with water molecule rotations around three symmetry axes whose partial contribution determines the band shape. As shown by detail studies [13, 15], the modes conserve their dominant role in the INS spectra of retained water, albeit are downshifted, when water molecules are coupled with the pore inner surface via hydrogen bonds. This very behavior is characteristic for the $G^{\rm wat}(\omega)$ spectrum in Fig. 3b. The three-ax partial contribution is sensitive to both chemical composition of the pore walls and the pore size [15]. Thus, the downshift of the red edge of the band from 550 to 320 cm^{-1} when going from the $G^{\rm ice}(\omega)$ spectrum to the $G^{\rm wat}(\omega)$ one highlights the shungite pore size of a few nm, which is well consistent with SANS data [19].

A clear vision of the chemical composition of the basic structural elements of shungite as well as of their five- and six-layer stacking obtained on the course of the current study has allowed suggesting both a model structure of an individual shungite globule and a globule involving 4 wt % water. A detailed discussion of globule models, based on rGO sheet and its stacks shown in Fig. 4, is presented in [21].

The performed neutron scattering study proved to be extremely effective and put the last point in the study of the structure and chemical composition of shungite. The rGO nature of the basic structural element, its size and chemical composition as well as five-six-layer stacking have received a direct experimental confirmation fully supporting the general concept on the shungite structure suggested earlier [3]. Both the linear size

of individual rGO sheets and the sheet stacks are responsible for the obtained L_{CSR} values of 1.5–2 nm. The stacks of such dimension form globules of $\sim$ 6 nm in size (the third level of structure) while the latter produce agglomerates of 20 nm and more (the forth level of structure) completing the fractal packing of shungite. The basic rGO fragments are hard reduced products of stable chemical composition due to which shungite presents a natural pantry of highly important raw material for the modern graphene technologies. It should be noted that presented study has concerned shungite of the highest carbon content from the Shun'ga deposits in Karelia. Shungites from other deposites differ quite considerably by both chemical composition and structural properties, on which strongly depends the area of their best applications.

Authors greatly appreciates financial support of RSF grants # 14-08-91376 (E. Sh.) and 13-03-00422 (N.R.) as well as the Basic Research Program, RAS, Earth Sciences Section-5 (N.R.).

1. J. Luo, J. Kim, and J. Huang, Acc. Chem. Res **46**, 2225 (2013).
2. C. K. Chua and M. Pumera, Chem. Soc. Rev. **43**, 291 (2014).
3. E. F. Sheka and N. N. Rozhkova, Int. J. Smart Nano Mat. **5**, 1 (2014).
4. N. N. Rozhkova, *Nanouglerod shungitov (Shungite Nanocarbon)*, Petrozavodsk, Karelian Research Centre of RAS (2011).
5. B. S. Razbirin, N. N. Rozhkova, E. F. Sheka, D. K. Nelson, and A. N. Starukhin, ZhETF **145**(5), 838 (2014).
6. L. Li, G. Wu, G. Yang, J. Zhao, and J.-J. Zhu, Nanoscale **5**, 4015 (2013).
7. I. Natkaniec, S. I. Bragin, J. Brankowski, and J. Mayer, in *Proc. ICANS XII Meeting, Abington 1993*, RAL Report 94-025 (1994), v. 1, p. 89.
8. M. Tagiri, J. Jpn. Assoc. Mineral. Petrol. Econ. Geol. **76**, 345 (1981).
9. G. I. Emel'yanova, L. E. Gorlenko, N. N. Rozhkova, M. N. Rumyantseva, and V. V. Lunin, Zh. Fiz. Khimii **84**, 1513 (2010).
10. E. L. Bokhenkov, I. Natkaniec, and E. F. Sheka, ZhETP **43**, 536 (1976).
11. P. G. Hall, A. Pidduck, and C. J. Wright, J. Colloid. Interfacr Sci. **79**, 339 (1981).
12. E. F. Sheka, V. D. Khavryutchenko, and I. V. Markichev, Usp. Khim. **64**, 419 (1995).
13. V. Crupi, D. Majolino, P. Migliardo, and V. Venuti, J. Phys. Chem. B **106**, 10884 (2002).
14. A. Buchsteiner, A. Lerf, and J. Pieper, J. Phys. Chem. B **110**, 22328 (2006).
15. C. Corsaro, V. Crupi, D. Majolino, S. F. Parker, V. Venuti, and U. Wanderlingh, J. Phys. Chem. A **110**, 1190 (2006).
16. E. F. Sheka, N. N. Rozhkova, I. Natkaniec, K. Holderna-Natkaniec, and K. Druzbicki, in *International Conference Advanced Carbon Nanostructures*, St. Petersburg, July 1-5 (2013), p. 69.
17. S. V. Tkachev, E. Yu. Buslayeva, A. V. Naumkin, C. L. Kotova, I. V. Laure, and S. P. Gubin, Neorganich. Mat. **48**, 909 (2012).
18. L. Stobinski, www.nanomaterials.pl (2014).
19. M. V. Avdeev, T. V. Tropin, V. L. Aksenov, L. Rosta, V. M. Garamus, and N. N. Rozhkova, Carbon **44**, 954 (2006).
20. E. Sheka and N. Popova, Phys. Chem. Chem. Phys. **15**, 13304 (2013).
21. E. F. Sheka, N. N. Rozhkova, I. Natkaniec, and K. Holderna-Natkaniec, arXiv:1403.4920 [cond-mat.mtrl-sci] (2014).